Rheologica Acta Rheol Acta 26:217–232 (1987)

Orientation and rheology of rodlike particles with weak Brownian diffusion in a second-order fluid under simple shear flow

C. Cohen, B. Chung, and W. Stasiak

School of Chemical Engineering, Cornell University, Ithaca, New York

Abstract: An analysis of particle orientation in a dilute suspension of rodlike particles in a second-order fluid was performed to examine the effects of the elasticity of the fluid and of weak Brownian diffusion of the particle on its orientation. Distributions of particle orientation under a simple shear flow with rate of shear g have been obtained as a function of a single nondimensional parameter, $\beta^* = \beta/r_e^2(D/g)$, which combines the effects of the particle aspect ratio r_e, the weak fluid elasticity β, and the weak Brownian rotation diffusion coefficient D of the particle. In the limit of large r_e, when the fluid elasticity is strong enough to overcome the rotational diffusion effect on the particle motion, most of the particles will orient close to the vorticity axis. A new shear-thinning mechanism of the shear viscosity of such systems is predicted by the theory.

Key words: Orientation, rodlike particle, weak Brownian diffusion, second-order fluid

1. Introduction

Suspension of rodlike particles in non-Newtonian fluids are important systems often encountered in polymer processing operations. Glass-fiber-filled thermoplastics are typical examples of such systems. The rheological behavior of the suspension is usually quite different from that of the suspending matrix. The orientation distribution of particles induced by the flow field strongly affects certain macroscopic physical properties such as the rheological behavior of the suspension which plays a crucial role during processing. It is therefore desirable to understand the effect of various parameters which may be varied during the processing in order to control fiber orientation [1–4]. It is still, however, a formidable task to model the real processing situations and obtain information about fiber orientation because of the complicated viscoelastic nature of the polymer matrix and the complex geometry of a processing situation. Many investigations have been reported in the literature concerning suspensions of rodlike particles in Newtonian fluids, and only a limited number of papers have addressed the problem of a non-Newtonian fluid matrix.

Jeffery [5] pioneered the investigation of the motion of rodlike particle in a flow field, and obtained the solution for the motion of spheroidal (or rodlike) particles in a Newtonian fluid undergoing a simple shear flow. Jeffery's solution indicated that a rodlike particle in a Newtonian fluid will rotate with respect to the vorticity axis periodically and indefinitely in one of an infinite family of orbits. The orbit for each particle is designated by an orbit constant C, which has a value between zero and infinity ($0 \leqq C \leqq \infty$). However, the distribution of particle orbits depends entirely on the initial distribution of orientation among the particles in the system. This leads to an "indeterminacy" of particle orientation for such a system which is the result of the assumption used in Jeffery's theory. Mason and his coworkers have carried out extensive theoretical and experimental investigations to search out the causes of the "indeterminacy" in Jeffery's solution since such "indeterminacy" is seldom found experimentally. They considered the following effects on particle orientations that were originally neglected by Jeffery: (1) fluid inertia [6]; (2) non-uniform shear field [7]; (3) non-uniform particle size distribution [8–11]; (4) particle interactions [12]; (5) particle Brownian motion [9, 13, 14]. All these investigations show that if any of the above effects is introduced, then an intrinsically preferred orientation will exist and a steady-state distribution independent of initial conditions will be reached. Aside from the extensive work of Mason's group, Leal and Hinch [15] have solved for the steady-state orientation distribution function by considering the effect of a weak Brownian motion of the particles, and Folger and Tucker have [16] recently obtained a steady-state orientation distribution function by introducing a particle-particle interation coefficient in concentrated fiber suspensions.

By comparison to the work on suspensions in a Newtonian matrix, there are relatively few studies concerning the be-

havior of rodlike particles in a non-Newtonian fluid. Saffman [17] was first to notice that rodlike particles will align along the vorticity axis ($C = 0$) under a Couette flow in a non-Newtonian fluid. Mason et al. [18–20] have done more extensive investigations for the particle motion in non-Newtonian media. Some detailed pictures about particle orbit drifting patterns were shown in their works. From their observation, they concluded also that the equilibrium orientation state for a rodlike particle in a non-Newtonian fluid is when the particle orients along the vorticity axis, where $C = 0$. Leal [21] considered the motion of rodlike slender particles in a weak viscoelastic fluid, the Rivlin-Ericksen second-order fluid, and obtained the particle angular velocities, $\dot{\theta}$ and $\dot{\phi}$, that describe the particle behavior in such a fluid. Brunn [22] has used a different approach to obtain similar results for dumbbell-like particles in a second-order fluid. From both of these studies, the particle motion is clearly affected by the fluid elasticity which leads to orbit drifting behavior of particles as was observed by Mason's group [19–20] and earlier by Saffman.

A dilute suspension of rodlike particles with weak Brownian diffusion in a second-order fluid under a simple shear flow is the subject of this paper. The orientation distribution of particles in such systems will be obtained from the solution of the generalized Fokker-Planck equation by utilizing Leal's result of particle angular velocities. The particle orientation distribution is affected by the combined effects of particle aspect ratio, weak Brownian diffusion of the particle, and weak fluid elasticity. When the fluid elasticity is strong enough to overcome the diffusion effect on the particle motion, most particles will orient close to the vorticity axis just as previously discussed for the single particle. The rheological properties of such a suspension will be calculated by using an approximate expression for the stress tensor [23]. A new shear-thinning mechanism of the shear viscosity of such systems is predicted by the theory.

The case of rodlike particles with strong Brownian diffusion (e.g. rodlike macromolecules) in a second-order fluid will be considered in a subsequent paper.

2. Theoretical background

2.1 Rodlike particle motion in a Newtonian fluid

Jeffery [5] has considered the motion of a single neutrally buoyant, spheroidal particle in a Newtonian fluid undergoing a simple shear flow. By assuming the absence of Brownian motion and by neglecting inertial forces for both the particle and the fluid, Jeffery obtained the equations of angular motion of the particle as

$$\dot{\theta} = \frac{g(r_e^2 - 1)}{(r_e^2 + 1)} \sin\theta \cos\theta \sin\phi \cos\phi \,, \tag{1}$$

$$\dot{\phi} = \frac{g}{(r_e^2 + 1)} (r_e^2 \cos^2\phi + \sin^2\phi) \,, \tag{2}$$

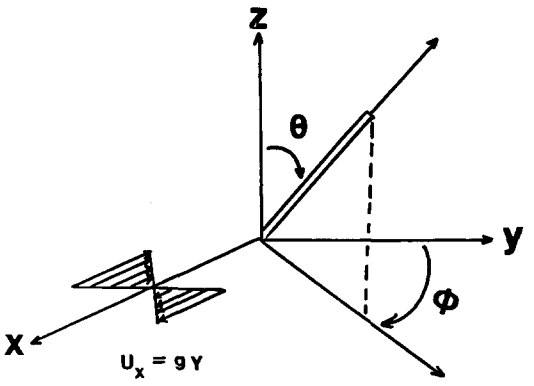

Fig. 1. The coordinate system

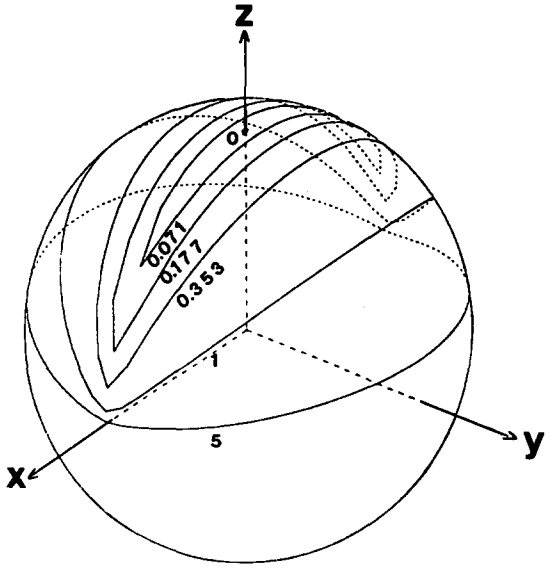

Fig. 2. 3-D representation of Jeffery orbits with different orbit constants (for particle aspect ratio $r_e = 16$)

where θ and ϕ are shown in figure 1, g is the velocity gradient in the y direction, and r_e is the equivalent aspect ratio of the particle. For particle shape other than spheroidal, as for example rods with circular or rectangular cross-section, r_e can be evaluated experimentally from the actual particle rotation period defined below [24].

Integration of eqs. (1) and (2) yields

$$\tan\theta = \frac{Cr_e}{(r_e^2 \cos^2\phi + \sin^2\phi)^{1/2}} \,, \tag{3}$$

$$\tan\phi = r_e \tan\left(\frac{2\pi t}{T} + \varkappa\right) \,, \tag{4}$$

where C and $\varkappa$ are integration constants. T is the period of one complete rotation of the particle with respect to

the vorticity axis (z-axis) and is given as

$$T = \frac{2\pi}{g}(r_e + r_e^{-1}) . \tag{5}$$

According to Jeffery's theory, a single spheroidal particle rotates in a periodic manner described by eqs. (3) and (4) for a given orbit constant C, and will stay in that orbit indefinitely as long as Jeffery's assumptions are not violated. The orbit constant C defines the three-dimensional ellipse traced out by the end of the particle on the surface of a sphere (see figure 2). The value of C is zero when the major axis of the particle is parallel to the vorticity axis and infinite when it lies in the plane of shear ($x-y$ plane). The particle rotates non-uniformly with respect to the z-axis (vorticity axis), and, for $r_e \gg 1$, it spends a time of order $r_e g^{-1}$ in the $x-y$ plane and then flips over in a time of order g^{-1}.

2.2 Rodlike particle motion in a second-order fluid

Among the limited theoretical studies in the literature about rodlike particles in non-Newtonian fluids, foremost is that of Leal [21] who studied the motion of slender rodlike particle in a Rivlin-Ericksen second-order fluid. The second-order fluid has a constant non-thinning shear viscosity like a Newtonian fluid, but has non-zero first and second normal-stress differences. The dimensionless stress expression of this continuum model can be written in a codeformational form as

$$\boldsymbol{T} = -P\boldsymbol{1} + \boldsymbol{Y}^{(1)} + \lambda[\boldsymbol{Y}^{(1)} \cdot \boldsymbol{Y}^{(1)} + \varepsilon_1 \boldsymbol{Y}^{(2)}] \tag{6}$$

where

$$\boldsymbol{Y}^{(1)} = \nabla \boldsymbol{U} + (\nabla \boldsymbol{U})^{\dagger}) \tag{7}$$

and

$$\boldsymbol{Y}^{(2)} = \frac{D}{Dt}\boldsymbol{Y}^{(1)} + \{(\nabla \boldsymbol{U}) \cdot \boldsymbol{Y}^{(1)} + \boldsymbol{Y}^{(1)} \cdot (\nabla \boldsymbol{U})^{\dagger}\} . \tag{8}$$

The superscript † indicates a transpose operation. The dimensionless parameter λ is defined as $(\psi_1 + \psi_2)\, U/l\eta_s$, where l and U are the characteristic length and velocity of the system, η_s is the fluid viscosity, and ψ_1 and ψ_2 are normal-stress coefficients defined below. The parameter λ is a measure of the intrinsic relaxation time, $(\psi_1 + \psi_2)/\eta_s$, of the viscoelastic fluid relative to the convective time scale of the flow, l/U. The parameter

$$\varepsilon_1 = -\frac{1}{2}\left(\frac{\psi_1}{\psi_1 + \psi_2}\right)$$

is related to the rheological parameters of the fluid, ψ_1 and ψ_2, which are defined in a simple shear flow by [25]

$$\psi_1 = \lim_{g_{yx} \to 0} \frac{\tau_{xx} - \tau_{yy}}{g_{yx}^2} , \tag{9}$$

$$\psi_2 = \lim_{g_{yx} \to 0} \frac{\tau_{yy} - \tau_{zz}}{g_{yx}^2} . \tag{10}$$

ψ_1 and ψ_2 are known as the zero-shear-rate first and second normal-stress coefficients, and g_{yx} is the velocity gradient. ψ_2 is usually much smaller than ψ_1 and has a negative sign [25].

In Leal's analysis, λ is considered to be small, $0 < \lambda \ll 1$, so that the constitutive equation (eq. (6)) is only slightly perturbed from that of a Newtonian fluid. This assumption limits the magnitude of the instantaneous non-Newtonian contributions to the particle's motion. Nevertheless, this small effect turns out to have a large cumulative influence on the particle orientation. Leal obtained the rate-of-change of the particle orientation in a second-order fluid under a simple shear flow as

$$\dot{\phi} \approx g(\cos^2\phi + r_e^{-2}) + \beta g \sin^2\theta \sin\phi \cos\phi (\sin^2\phi - \cos^2\phi) + \ldots , \tag{11}$$

$$\dot{\theta} \approx g \sin\theta \cos\theta \sin\phi \cos\phi - 2\beta g \sin^3\theta \cos\theta \sin^2\phi \cos^2\phi + \ldots , \tag{12}$$

where $\beta = -(g\psi_2)/(8\eta_s)$ is of order λ and hence $\beta \ll 1$. β characterizes the non-Newtonian effects on the particle orientation in eqs. (11) and (12). If ψ_2 is zero, $\beta = 0$ and the particle motion reduces to that in a Newtonian fluid.

From Jeffery's solution, one can define the orbit constant and phase angle by integrating eqs. (1) and (2) to obtain

$$C = \tan\theta \left(\frac{1}{r_e^2}\sin^2\phi + \cos^2\phi\right)^{1/2} , \tag{13}$$

$$\tau = \tan^{-1}\left(\frac{1}{r_e}\tan\phi\right) . \tag{14}$$

The orbit constant C appears in eq. (3) as a constant of integration in the case of a Newtonian fluid and thus $dC/dt = 0$; for the second-order fluid, on the other hand, one gets from eqs. (11) and (12) that [21]

$$\frac{dC}{dt} \approx -\beta g \sin^2\theta \sin^2\phi C \quad (\text{for } r_e \gg 1) . \tag{15}$$

A unique feature of the above theoretical results is the orbital drift of the particle in a second-order fluid. The rodlike slender particle will drift through Jeffery's orbits to the preferred orbit $C = 0$, which means that the particle will eventually orient along the vorticity

axis. The rate of drifting is characterized by βg and depends therefore on the magnitude of the β parameter. This orbital drifting behavior had been observed earlier by Saffman [17], Karnis and Mason [18], and subsequently confirmed by Gauthier et al. [19], and Bartram and Mason [20] in their experimental investigations of the motion of rodlike particles in a non-Newtonian fluid.

3. Orientation and rheology of rodlike particles in a second-order fluid

The hydrodynamic motion of a single rodlike particle with no Brownian motion in a Newtonian fluid or a viscoelastic fluid subjected to a simple shear flow were reviewed in the previous section. We consider here the effect of weak Brownian diffusion of rodlike particles on their orientation in a second-order fluid. The analogous effect for a Newtonian matrix was considered by Leal and Hinch [15] and their results are summarized below. To determine the bulk properties of a suspension consisting of many non-interacting particles in the suspending fluid, the distribution of orientation among all the suspended particles is needed. This distribution can be obtained by first calculating the time-average distribution of orientation for each particle orbit, and then by specifying the statistical distribution of orbits among the particles [15]. The latter is especially difficult to achieve.

The distribution function of particles orientation f is governed by the Fokker-Planck equation

$$\frac{\partial f}{\partial t} + \nabla \cdot (g\,\omega f) = \nabla \cdot (D \nabla f)\,, \tag{16}$$

where $g\,\omega$ is the angular velocity caused by hydrodynamic forces, and D is the particle rotational Brownian diffusion coefficient, which is a constant in a dilute suspension. The term $\nabla \cdot (g\,\omega f)$ is the convective term describing the rate of change of the distribution function resulting from the deterministic change of the distribution function, and $\nabla \cdot (D \nabla f)$ is the diffusive term due to the diffusion process induced by a gradient in the probability distribution.

Since the action of particle rotational Brownian motion has a randomizing effect on the particle orientation, the final steady-state distribution of orientation represents a compromise between the anisotropic periodical orientation associated with undisturbed Jeffery orbits and the uniform orientation which results from unopposed random Brownian motion. For a large rodlike particle the particle Brownian motion is weak but its effect will produce a steady state equilibrium distribution orientation after a sufficiently long time (order of $(D r_e^2)^{-1}$) [26]. Hinch and Leal [27] have obtained a perturbation solution to the steady-state form of eq. (16) in terms of the small parameter, D/g, and the zeroth-order solution, f_0, can be expressed in the following form

$$f_0(C, \tau) = l(C)\, g(C, \tau)\,, \tag{17}$$

where C and τ correspond to the orbit constant and phase angle defined in eqs. (13) and (14). In particular, $g(C, \tau)$ describes the phase-angle distribution around each specific orbit and is given by:

$$g(C, \tau) = \frac{1}{C r_e} [1 + C^2(\cos^2\tau + r_e^2 \sin^2\tau)]^{3/2} \tag{18}$$

where $C \neq 0$.

On the other hand, $l(C)$ is the distribution function of orbit constants and has the following asymptotic form for $r_e \gg 1$:

$$l(C) \approx \frac{1}{\pi} \frac{C}{(4C^2 + 1)^{3/2}}\,. \tag{19}$$

The product of these two functions gives the overall orientation distribution of particles in the suspension. In terms of (θ, ϕ) coordinates, this steady-state distribution is [27]

$$f_0(\theta, \phi) \cong \frac{1}{\pi r_e} [4 \sin^2\theta (\cos^2\phi + r_e^{-2} \sin^2\phi) + \cos^2\theta]^{-3/2}\,. \tag{20}$$

Rodlike particles with weak Brownian motion in a second-order fluid will be discussed in the following section, where it will be shown that eq. (20) is a special case of a more general solution. It will be necessary to examine first the validity and limitation of the Fokker-Planck equation (eq. (16)) for the case of a relaxing non-Newtonian matrix.

3.1 The governing equation and its solution

The assumption that enters in the derivation of the Fokker-Planck equation for the probability density f and that must be of concern here is the assumption that the macroscopic Brownian particle is subjected to random stochastic forces which are totally uncorrelated in time (on the macroscopic time scale). If this assumption is satisfied, the fluctuating forces are then said to follow a Markovian process and the drag on the particle which is related to the autocorrelation of the fluctuating force by the fluctuation-dissipation theorem is then independent of time [28]. Otherwise, the "memory" of the molecular impacts received by the particle during a given interval of time is not "completely lost" causing the drag and hence the diffusion coefficient of

the particle to be time dependent. We can assume that the form of the Fokker-Planck equation as written in eq. (16) remains unchanged, but that in a relaxing fluid we have to consider the time dependence of D. Support for this assumption comes from the fact that a molecular derivation of hydrodynamic equations for a binary mixture yields the classical convection-diffusion equation for the concentration equation with a diffusion coefficient which in general will be time (or frequency) dependent [29].

Let us now consider the condition for which the time (or frequency) dependence of the diffusion coefficient is negligible. Volkov and Vinogradov [30] have recently shown that for a Maxwell fluid with a relaxation time τ, the drag kernel $\xi(t)$ on a bead of radius a may be expressed as

$$\xi(t) = \xi \tau^{-1} e^{-1/\tau} \quad \text{for } t \geqq 0 ,$$

where $\xi = 6\pi\eta a$. Taking the Fourier transform of the above equation, one obtains for the real part:

$$\xi(\omega) = \xi(1 + \omega^2\tau^2)^{-1} .$$

Hence, in the Maxwell model and in the analogous second-order fluid we must determine the magnitude of $\omega\tau$ compared to unity to establish the magnitude of the frequency contribution term to the drag coefficient or diffusion coefficient. Since we are considering here the effect of rotation diffusion on the orientation distribution, the time scale (or frequency) of interest must be of the order of D^{-1} (or D); hence, taking

$$\omega \sim D$$

we must assume $D\tau \ll 1$ to legitimize $\xi(\omega) \to \xi$ and $D \to$ constant. For the case under consideration, the assumption $D\tau \ll 1$ will, however, be automatically incorporated into model as the perturbation scheme in the second-order fluid requires that β and hence τg be less than unity (where $\tau = -\psi_2/8\eta_s$) and the weak Brownian diffusion limit requires that D/g be less than unity. Therefore, since $\tau g \ll 1$ and $D/g \ll 1$, the condition that $D\tau \ll 1$ is automatically satisfied, and we can assume a constant D in eq. (16).

The convective motion of a single rodlike particle in a second-order fluid undergoing a simple shear flow described in section 2.2 can be written as [21, 22]:

$$\boldsymbol{\omega} = \boldsymbol{\omega}_0 + \beta\boldsymbol{\omega}_1 , \tag{21}$$

where $\boldsymbol{\omega}_0$ is Jeffery's solution for a Newtonian fluid, and $\beta\boldsymbol{\omega}_1$ is the additional contribution caused by the elasticity of the second-order fluid as given in eqs. (11) and (12). Substitution of eq. (21) into the Fokker-Planck equation (eq. (16)) yields the following governing equation for the distribution function under steady-state and constant D conditions:

$$\nabla \cdot (\boldsymbol{\omega}_0 + \beta\boldsymbol{\omega}_1) f = \frac{D}{g} \nabla^2 f . \tag{22}$$

In the limit of weak Brownian diffusion, which means $D/g \ll 1$, one can expand the solution in terms of this small parameter as

$$f = f_0 + \left(\frac{D}{g}\right) f_1 + \left(\frac{D}{g}\right)^2 f_2 + \dots , \tag{23}$$

one then obtains the following equation by substituting eq. (23) into eq. (22)

$$\begin{aligned} &\nabla \cdot (\boldsymbol{\omega}_0 f_0) + \left(\frac{D}{g}\right) \nabla \cdot (\boldsymbol{\omega}_0 f_1) + \left(\frac{D}{g}\right)^2 \nabla \cdot (\boldsymbol{\omega}_0 f_2) + \dots \\ &\quad + \beta^* r_e^2 \left(\frac{D}{g}\right) \nabla \cdot (\boldsymbol{\omega}_1 f_0) + \beta^* r_e^2 \left(\frac{D}{g}\right)^2 \nabla \cdot (\boldsymbol{\omega}_1 f_1) + \dots \\ &= \left(\frac{D}{g}\right) \nabla^2 f_0 + \left(\frac{D}{g}\right)^2 \nabla^2 f_1 + \dots , \end{aligned} \tag{24}$$

where $\beta^* = \beta/[r_e^2(D/g)]$. The parameter β^* will be discussed in details later. The governing equation to zeroth order is then given by

$$\nabla \cdot \boldsymbol{\omega}_0 f_0 = 0 . \tag{25}$$

After coordinate transformations from the (θ, ϕ) system to the (C, τ) systems, eq. (25) can be solved as

$$f_0(C, \tau) = l(C)\, g(C, \tau) \tag{26}$$

which has the same form as in the Newtonian case. It may be deduced from eq. (25) that the solution for $g(C, \tau)$ is the same as eq. (18), but that the function $l(C)$ is yet to be determined.

Since both the diffusion and elasticity effects on the distribution function are lost in eq. (25), one can follow arguments similar to those used by Leal and Hinch [15] to recover this information by integrating eq. (22) and making use of the divergence theorem. This results in

$$\oint (\boldsymbol{\omega} f) \cdot \boldsymbol{n}\, ds = \frac{D}{g} \oint (\nabla f) \cdot \boldsymbol{n}\, ds . \tag{27}$$

Substitution of eq. (21) yields

$$\oint [(\boldsymbol{\omega}_0 + \beta\boldsymbol{\omega}_1) f] \cdot \boldsymbol{n}\, ds = \frac{D}{g} \oint (\nabla f) \cdot \boldsymbol{n}\, ds . \tag{28}$$

Further, if one chooses the Jeffery orbit as the line integral domain, then $\boldsymbol{\omega}_0 \cdot \boldsymbol{n} = 0$. When the expanded

form of f in eq. (23) is used, eq. (28) becomes

$$\beta^* r_e^2 \left(\frac{D}{g}\right) \oint \left\{\omega_1 \left[f_0 + \left(\frac{D}{g}\right) f_1 + \left(\frac{D}{g}\right)^2 f_2 + \ldots\right]\right\} \cdot \boldsymbol{n}\, ds$$

$$= \left(\frac{D}{g}\right) \oint \left\{\nabla \left[f_0 + \left(\frac{D}{g}\right) f_1 + \left(\frac{D}{g}\right)^2 f_2 + \ldots\right]\right\} \cdot \boldsymbol{n}\, ds \quad (29)$$

and gives the "order one" equation as

$$\beta^* r_e^2 \oint (\omega_1 f_0) \cdot \boldsymbol{n}\, ds = \oint (\nabla f_0) \cdot \boldsymbol{n}\, ds\,. \quad (30)$$

To obtain the distribution of orbits, $l(C)$, one has to use eq. (30). Notice that when $\beta^* = 0$, i.e. no fluid elasticity, eq. (30) will reduce to the condition used by Leal and Hinch for the Newtonian fluid case. After lengthy algebra (see Appendix A), substitution of eq. (26) into eq. (30) will give

$$l(C) = \text{const}\, C^{J_1(r_e,\beta^*)} \left[\frac{HC^4 + KC^2 + M}{H}\right]^{J_2(r_e,\beta^*)}$$

$$\times \left[\frac{2HC^2 + K - \Delta^{1/2}}{2HC^2 + K + \Delta^{1/2}}\right]^{J_3(r_e,\beta^*)} \cdot F_0(C) \cdot F_1(C) \cdot F_2(C)\,, \quad (31)$$

where

$$J_1(r_e,\beta^*) = 1 - \frac{2\beta^* r_e^4}{(r_e^2-1)^2}\,, \quad (32)$$

$$J_2(r_e,\beta^*) = -\frac{3}{4} + \frac{\beta^* r_e^4}{2(r_e^2-1)^2}\,, \quad (33)$$

$$J_3(r_e,\beta^*) = \frac{(\frac{3}{4}K - 3)}{\Delta^{1/2}} - \frac{1}{2}\frac{(r_e^2+1)^2(\beta^* r_e^2)}{(r_e^2-1)^2\Delta^{1/2}} + \frac{K\beta^* r_e^4}{2(r_e^2-1)^2\Delta^{1/2}}\,, \quad (34)$$

$$H(r_e) = r_e^2 + 1\,, \quad (35)$$

$$K(r_e) = \frac{1}{4}r_e^2 + \frac{7}{2} + \frac{1}{4r_e^2}\,, \quad (36)$$

$$M(r_e) = (r_e^2+1)/r_e^2\,, \quad (37)$$

$$\Delta = K^2 - 4HM\,. \quad (38)$$

The function $F_0(C)$ is given by

$$F_0(C) = \left[\frac{C^2}{2 + (1+r_e^2)C^2 + 2\sqrt{R(C^2)}}\right]^{Y_0(r_e,\beta^*)}, \quad (39)$$

where

$$Y_0(r_e,\beta^*) = \frac{\beta^* r_e^4}{(r_e^2-1)^2} \quad (40)$$

and

$$R(x) = 1 + (1+r_e^2)x + r_e^2 x^2\,. \quad (41)$$

The formulae for $F_i(C)$ $(i = 1, 2)$ are given by:

$$F_i(C) = \exp\left[-Y_i \tan^{-1}\left(\frac{2 + (1+r_e^2)x_i + (1+r_e^2+2r_e^2x_i)C^2}{2\sqrt{-R(x_i)}\cdot\sqrt{R(C^2)}}\right)\right], \quad (42)$$

where

$$x_{1,2} = -\frac{1}{2H}[K \pm \sqrt{\Delta}]\,, \quad (43)$$

$$Y_{1,2} = -\frac{\beta^* r_e^4}{(r_e^2-1)^2} \cdot \left[1 \mp \frac{K}{\sqrt{\Delta}}\right] \cdot \sqrt{-R(x_{1,2})}\,. \quad (44)$$

The analytic continuation of (42) when $R(x_i) > 0$ is given by:

$$F_i(C) = \left[\frac{C^2 - x_i}{2 + (1+r_e^2)x_i + (1+r_e^2+2r_e^2x_i)C^2 + 2\sqrt{R(x_i)R(C^2)}}\right]^{\bar{Y}_i}, \quad (45)$$

where

$$\bar{Y}_{1,2} = \frac{\beta^* r_e^4}{(r_e^2-1)}\left[1 \mp \frac{K}{\sqrt{\Delta}}\right]\sqrt{R(x_{1,2})}\,. \quad (46)$$

For large r_e the numerical value of the coefficient x_1 tends to -0.25 and $R(x_1) < 0$, while x_2 tends to 0 and $R(x_2) > 0$. Therefore for large r_e, $F_1(C)$ takes the functional form (42) and $F_2(C)$ is given by (45). In the limit $r_e \gg 1$ eq. (31) can be simplified to

$$l(C) \approx \text{const}\,(4C^2+1)^{2\beta^* - 1.5}\, C^{1-4\beta^*}\,, \quad (47)$$

where the constant can be determined by using the normalization condition [15]

$$\int_0^\infty I(C)\,dC = \frac{1}{4\pi}. \tag{48}$$

Again, for $\beta^* = 0$, i.e. in the absence of fluid elasticity, eq. (47) will reduce back to eq. (19) of the Newtonian case.

The mechanism of the approach to the steady state distribution of orbits among the particles in a second-order fluid is different from that in a Newtonian fluid. In the latter, the Brownian diffusion, which is a random process, is the only force that alters the orbit of a particle. In addition to the diffusion force, the elasticity of a second-order fluid will also change the orbit of a particle, and this effect will drive the particles toward the vorticity axis, $C = 0$. Since Brownian diffusion is a randomizing force, it will oppose the fluid elasticity force and the net effect will give a steady state distribution of orbits which is a compromise between the distribution of particles with weak diffusion in a Newtonian fluid, which is essentially along the flow direction, and a delta peak orientation along the vorticity axis.

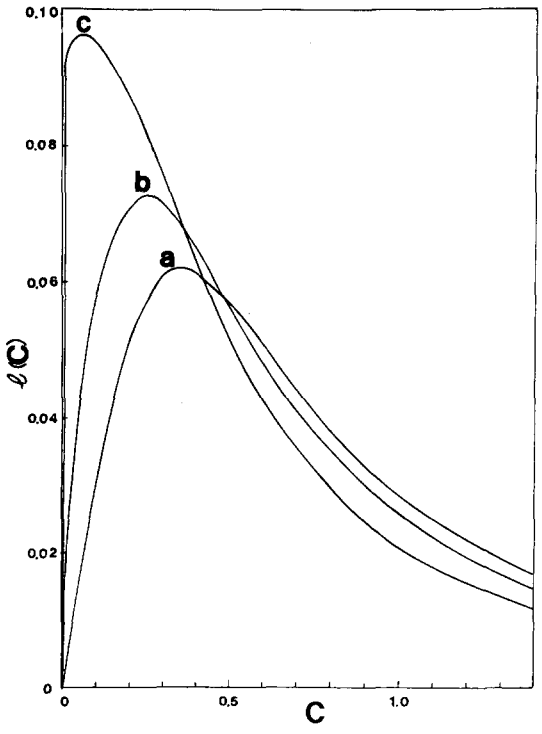

Fig. 3. Orbit constant distribution function $I(C)$ versus orbit constant C for different values of β^* with $r_e = 16$: (a) $\beta^* = 0$, (b) $\beta^* = 0.125$, (c) $\beta^* = 0.24$

3.2 *Distribution of orientation*

Eq. (47) is valid for large r_e, with the exception of a small region of order $(1/r_e)$ in the vicinity of $C = 0$, where for $\beta^* > 0.25$ it is divergent for $C \to 0$. To obtain the approximate solution in this region one has to expand the full solution (31) around $C = 0$. We find easily that up to the first order in C: $I(C) \sim C$. That means that for very small values of C, corresponding to the particles oriented towards the vorticity axis, the influence of the non-Newtonian properties of the solvent is not felt, i.e. the form of the distribution function $I(C)$ does not depend on β^*. As a result of the Brownian diffusion the number of particles oriented along the vorticity axis is equal to zero [$I(C) \to 0$ for $C \to 0$] as it is in a Newtonian fluid [15]. Note that Leal's result of the drift of particles through Jeffery's orbits towards the preferred orbit $C = 0$ [see eq. (15)], leading to the Dirac's delta function for the steady-state equilibrium distribution over orbits, is not recovered as in our regime of small β and small D/g, we cannot take D/g to zero without simultaneously taking β to zero [see eq. (29)].

The parameter β^* $(= \beta/r_e^2(D/g))$ is a measure of the relative influence of the fluid elasticity to the particle Brownian motion on the particle orientation. These two effects, assumed to be both weak, will balance to lead to a steady-state distribution of orbits. When β^* increases, the elasticity term of the hydrodynamic force is becoming larger, and the distribution of orbits will shift toward $C = 0$, the most stable orientation for non-Brownian rodlike particles in the viscoelastic fluid. An estimation of the distribution over orbits is indicated in figure 3. For simplicity it is limited to the asymptotic limit of large r_e using the expression in eq. (47) which is limited to $\beta^* < 0.25$ as it does not reproduce the correct limiting behavior given by the full solution of eq. (42) in the region of very small C when $\beta^* > 0.25$. The function $I(C)$ has a sharp maximum which becomes sharper and shifts toward $C = 0$ with growing β^*. This means that most of the particles start to orient closer to the vorticity axis $C = 0$ with increasing fluid elasticity. It is clear that the asymptotic limit given by eq. (47) will not be able to describe the "boundary layer" region around $C = 0$ as β^* increases beyond 0.25 for which one needs the full solution (42).

As indicated in eq. (26), the complete picture of particle orientation is given by $f_0(C, \tau)$ as the product of $g(C, \tau)$ and $I(C)$. One can transform the distribution function, f_0, from the (C, τ) coordinate system back to

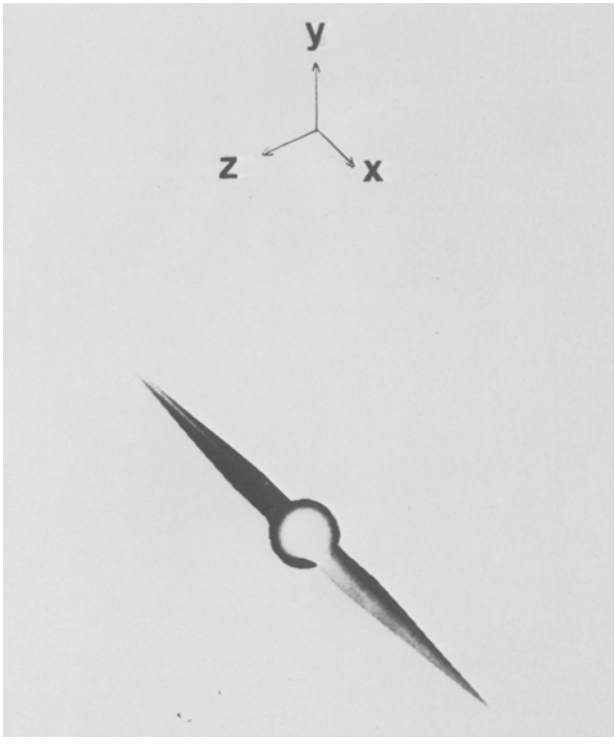

Fig. 4. 3-D representation of the orientation distribution function in a Newtonian fluid under a simple shear flow field ($\beta^* = 0$, $r_e = 16$). x designates the flow direction and z the vorticity axis

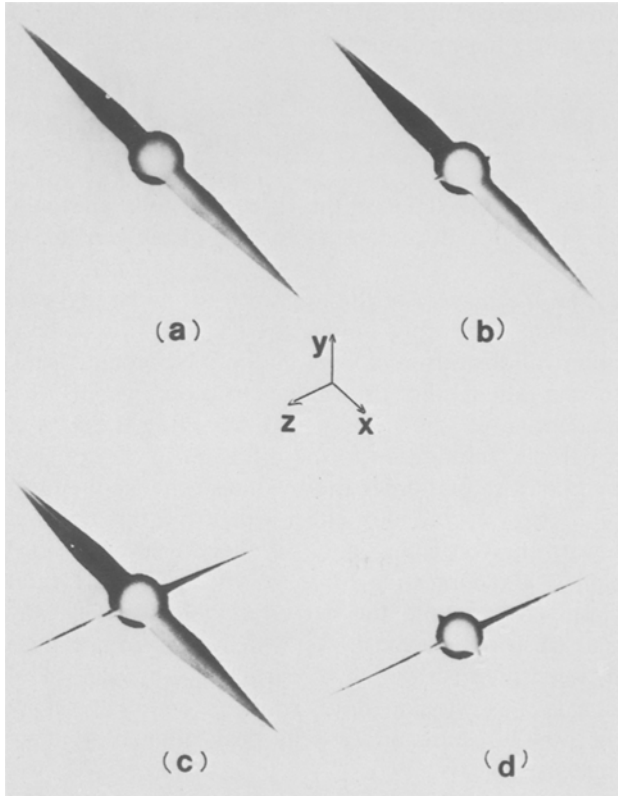

Fig. 5. 3-D representation of the orientation distribution function in a second-order fluid under a simple shear flow field ($r_e = 16$): (a) $\beta^* = 1/32$, (b) $\beta^* = 1/16$, (c) $\beta^* = 1/8$, (d) $\beta^* = 3/16$. x designates the flow direction and z the vorticity axis

(θ, ϕ) to obtain

$$f_0(\theta,\phi) = \text{const}\left\{r_e\left[4\sin^2\theta\left(r_e^{-2}\sin^2\phi+\cos^2\phi\right)+\cos^2\theta\right]\right\}^{-3/2} \times\left\{4+\frac{1}{\tan^2\theta\,(r_e^{-2}\sin^2\phi+\cos^2\phi)}\right\}^{2\beta^*}. \quad (49)$$

From eq. (31) the distribution of orbits $l(C)$ is zero at $C = 0$ indicating that there are no particles with this orbit constant. When particles have an orientation $\theta = 0$, or π, they have a particle orbit constant corresponding to $C = 0$ and as a result (see Appendix A),

$$f_0(\theta,\phi) = l(C) = 0\,, \quad \text{at } \theta = 0, \pi\,. \quad (50)$$

The constant in eq. (49) can be determined for each specific β^* value, and one can therefore actually plot the distribution function, f_0, in a 3-D spherical coordinate system.

Figure 4 represents the results of $f_0(\theta, \phi)$ for the Newtonian case, $\beta^* = 0$. As shown in the figure, the highest probability of orientation at steady state is in the flow direction (x-axis). The probability of orientation in other directions is non-zero but very small (except for $\theta = 0$ and π where it is zero) and is represented by a uniform sphere which is *not drawn to scale* to make it visible on the figure. The z-axis is the vorticity axis and one can watch how the orientation develops near this direction as a function of β^* by proceeding to the following figures.

For $\beta^* = 1/32$, figure 5a, the elasticity effect is still too small to show any obvious change in the distribution function compared to that of the Newtonian case. In figure 5b, $\beta^* = 1/16$, the major orientation is still in the flow direction, but there is a small peak now appearing near the z-axis. This means that the elasticity has brought some of the particles to orient close to the vorticity axis. As β^* increases further to 1/8, the effect of the fluid elasticity on the orientation distribution is now clearly seen in figure 5c. The peaks near the z-axis are getting larger at the expense of the peaks along the x-direction. In the case of $\beta^* = 3/16$, shown in figure 5d, the major orientation is close to the vorticity axis (z-axis). The fluid elasticity is now the domi-

nant effect on the orientation of the particles as most of the particles are oriented along the vorticity axis.

3.3 Calculations of rheological properties

Theoretically, once the distribution of orientation of the particles in a suspension is determined, one should be able to evaluate any physical property of the system which is dependent on particle orientation as long as a suitable expression to describe that property is available or can be obtained. To describe the rheological behavior of a dilute suspension of rodlike particles in a second-order fluid, one needs an expression for the bulk stress pertaining to this system. A suspension is a system which is determined only in a statistical sense because the exact location and orientation of the particles are different for different realizations of the suspension with the same macroscopic conditions. Many such realizations with the same macroscopic boundary conditions make up an ensemble. Batchelor [23] has defined the bulk stress of such a system as an average over an ensemble or realizations. This average represents an integration over a suitably chosen volume of ambient fluid and particles together when the suspension is statistically homogeneous. In other words, the chosen volume should have a characteristic length l such that the volume l^3 is large enough to contain a statistically significant number of particles while l is still small compared to the characteristic length scale of the bulk flow field. The bulk stress of the suspension has meaning only in the above "average" sense.

Batchelor [23] has discussed extensively the bulk stress of a suspension resulting from a pure hydrodynamic force in a Newtonian fluid. Later, Hinch and Leal [26] employed his results to express the bulk stress in terms of statistical averages:

$$\frac{\sigma_{12}^H}{\Phi g \eta_s} = A\langle \sin^4\theta \sin^2 2\phi\rangle + 2B\langle \sin^2\theta\rangle + 2, \tag{51}$$

$$\frac{\sigma_{11}^H - \sigma_{22}^H}{\Phi g \eta_s} = -A\langle \sin^4\theta \sin 4\phi\rangle, \tag{52}$$

$$\frac{\sigma_{22}^H - \sigma_{33}^H}{\Phi g \eta_s} = \frac{A}{2}\langle \sin^4\theta \sin 2\phi\rangle - 2(A-B)\langle \sin^2\theta \sin 2\phi\rangle, \tag{53}$$

where g is the shear rate, η_s is the viscosity of the ambient fluid, and Φ is the volume fraction of suspended particles. When $r_e \gg 1$,

$$A = \frac{r_e^2}{4(\ln 2r_e - 1.5)}, \tag{54}$$

$$B = \frac{3\ln 2r_e - 5.5}{r_e^2}. \tag{55}$$

The angle-bracket average is defined as

$$\langle P(\theta,\phi)\rangle = \int_0^{\pi} d\theta \int_0^{2\pi} \sin\theta\, P(\theta,\phi) f(\theta,\phi)\, d\phi, \tag{56}$$

where $f(\theta,\phi)$ is the orientation distribution function.

However, the hydrodynamic force is not the only source to contribute to the particle stress. In some cases, other sources, such as Brownian force, electric force, etc., also affect the particle motion so as to contribute to the particle stress directly. These direct contributions should also be included (Kirkwood and Auer [31], Saito [32], and Brenner [33]). In our system, the two contributions to the stress are the hydrodynamic force and the Brownian force; hence, the particle stress can be written as

$$\sigma_{ij}^P = \sigma_{ij}^H + \sigma_{ij}^D. \tag{57}$$

Giesekus [34] and Hinch and Leal [26] have shown that

$$\frac{\sigma_{12}^D}{\Phi g \eta_s} = \left(\frac{D}{g}\right) F\langle \sin^2\theta \sin 2\phi\rangle, \tag{58}$$

$$\frac{\sigma_{11}^D - \sigma_{22}^D}{\Phi g \eta_s} = -\left(\frac{D}{g}\right) 2F\langle \sin^2\theta \cos 2\phi\rangle, \tag{59}$$

and

$$\frac{\sigma_{22}^D - \sigma_{33}^D}{\Phi g \eta_s} = \left(\frac{D}{g}\right) F\{3\langle \sin^2\theta\rangle - 2 + \langle \sin^2\theta \cos 2\phi\rangle\}, \tag{60}$$

where D is the rotational Brownian diffusion coefficient, and when $r_e \gg 1$, F may be taken as

$$F = \frac{3r_e}{(\ln 2r_e - 0.5)}. \tag{61}$$

When a particle is in a second-order fluid, the particle motion caused by purely hydrodynamic forces consist of two parts: the Newtonian part and an additional contribution due to the elasticity of the fluid; hence σ_{ij}^H could be written in terms of two components, and eq. (57) can be modified as

$$\sigma_{ij}^P = \sigma_{ij}^{HN} + \sigma_{ij}^{HE} + \sigma_{ij}^D, \tag{62}$$

where σ_{ij}^{HN} and σ_{ij}^D have the same expressions as those for the particles in a Newtonian medium, and σ_{ij}^{HE} is the additional direct contribution from the elasticity. Kaloni and Stastna [35] have obtained an expression for σ_{ij}^{HE} for spherical particles in a second-order fluid. For the relatively more complicated geometry of rodlike particles (in a second-order fluid) there are no available expressions for σ_{ij}^{HE} and no attempts to obtain such an expression will be made here. The complete particle stress expression that describes the rodlike par-

ticle in a second-order fluid is therefore not available, but we shall discuss the contribution from each term in eq. (62) and show that in the present case both σ_{ij}^{HE} and σ_{ij}^{D} are expected to be negligible compared to σ_{ij}^{HN}.

For rodlike particles with weak Brownian diffusion in a Newtonian fluid, Hinch and Leal [26] have solved the orientation distribution function to order (D/g) and obtained expressions for both f_0 and f_1 where

$$f = f_0 + \left(\frac{D}{g}\right) f_1 . \tag{63}$$

By using eq. (63), they found the particle contribution of σ_{12}^{HN} and σ_{12}^{D} to be

$$\sigma_{12}^{HN} \sim \Phi \eta_s g \left\{0.315 \frac{r_e}{\ln r_e}\right\} , \tag{64}$$

$$\sigma_{12}^{D} \sim \Phi \eta_s g \left\{O\left(\frac{D}{g}\right)^2\right\} \tag{65}$$

while, for the particle normal-stress difference, $(\sigma_{11}^{P} - \sigma_{33}^{P})$, the contribution from $(\sigma_{11}^{HN} - \sigma_{33}^{HN})$ and $(\sigma_{11}^{D} - \sigma_{33}^{D})$ are

$$(\sigma_{11}^{HN} - \sigma_{33}^{HN}) \sim \Phi \eta_s g \left\{\frac{D}{g}\left(\frac{r_e^4}{4 \ln r_e}\right)\right\} , \tag{66}$$

$$(\sigma_{11}^{D} - \sigma_{33}^{D}) \sim \Phi \eta_s g \left\{\frac{D}{g}\left(\frac{16 r_e}{\ln r_e}\right)\right\} . \tag{67}$$

Similar results were obtained for $(\sigma_{22}^{P} - \sigma_{33}^{P})$. Eqs. (64–67) show that it is legitimate to neglect the σ_{ij}^{D} term from eq. (53) when Brownian diffusion is weak and $r_e \gg 1$.

For spherical particles in a second-order fluid, Kaloni and Stastna [35] found that σ_{ij}^{HE} will not make any contribution to the shear stress, but will have a contribution of $O(\lambda)$ to the normal stresses, where λ has been defined earlier as $(\psi_2 + \psi_1) U/l\eta_s$. In our case, this contribution will be small compared to the $O(\beta^*)$ effect retained in σ^{HN} when $r_e^2 D/g$ is small and will therefore be negligible for D sufficiently small. Further evidence will be given in a subsequent paper where an expression for σ_{ij}^{P} of rodlike particles with strong Brownian motion in a second-order fluid will be derived; it will be shown that, in this case, σ_{ij}^{HE} is about at least one order of magnitude smaller than σ_{ij}^{HN} when the fluid elasticity is weak. We shall therefore assume that this term is also negligible in the particle stress expression of eq. (62) for small elasticity effects. The dominant contribution to the stress expression for large rodlike particle in a second-order fluid will then be taken as σ_{ij}^{HN}; and although we neglect the direct contributions to the particle stress caused by weak fluid elasticity and Brownian diffusion, σ_{ij}^{HN} must, of course, be evaluated on the basis of the distribution of particle orientations which is governed by these effects. Consequently, these to weak forces of Brownian diffusion and fluid elasticity will make indirect contributions to the particle stress by virtue of their influences on the distribution of particle orientations. In other words, the particle stress must be evaluated according to eqs. (51–53) with the orientation distribution function which has been obtained in eq. (49).

The resulting non-dimensional shear viscosity decreases as β^* increases as shown in figure 6. Gauthier et al. [19] have used the stress expression of eq. (51) to calculate the intrinsic viscosity,

$$[\eta] = \lim_{\Phi \to 0} \frac{\eta - \eta_s}{\Phi \eta_s} \tag{68}$$

based on the experimentally observed orientation distribution; they find that the intrinsic viscosity of the non-Newtonian suspension is lower than that in the Newtonian system for the same particle size. From the analysis presented here, this behavior could be due to the fact that when β^* increases, more particles will orient close to the vorticity axis leading to a decrease in the viscosity of the system.

The dependence of the shear viscosity on the particle aspect ratio is also shown in figure 6: The entire viscosity curve is higher for a suspension of particles with larger aspect ratios.

The calculations for eqs. (52) and (53) show that the contributions from particles to the first and second normal-stress differences are very small, for example, $(\sigma_{11}^{HN} - \sigma_{22}^{HN})/\Phi g \eta_s$ has the value of order 10^{-4} for $r_e = 50$. $(\sigma_{22}^{HN} - \sigma_{33}^{HN})/\Phi g \eta_s$ is about two orders of

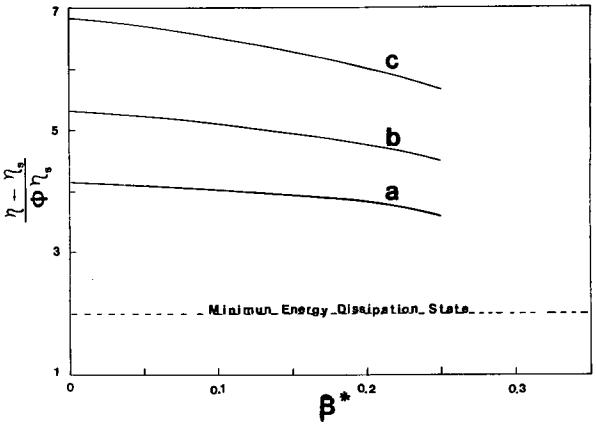

Fig. 6. Non-dimensional shear viscosity, $(\eta - \eta_s)/\Phi \eta_s$, of a suspension of rodlike particles with weak Brownian diffusion in a second-order fluid as a function of β^* and r_e: (a) $r_e = 15$, (b) $r_e = 30$, (c) $r_e = 50$

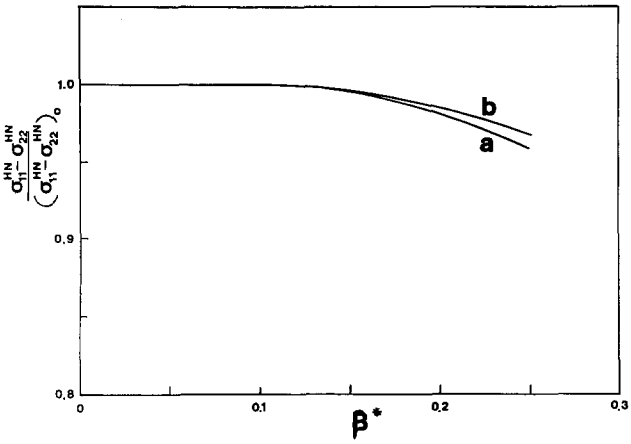

Fig. 7. Normalized first normal-stress difference, $(\sigma_{11}-\sigma_{22})^{HN}/(\sigma_{11}-\sigma_{22})_0^{HN}$, of a suspension of rodlike particles with small D in a second-order fluid as a function of β^* and r_e: (a) $r_e = 50$, (b) $r_e = 16$

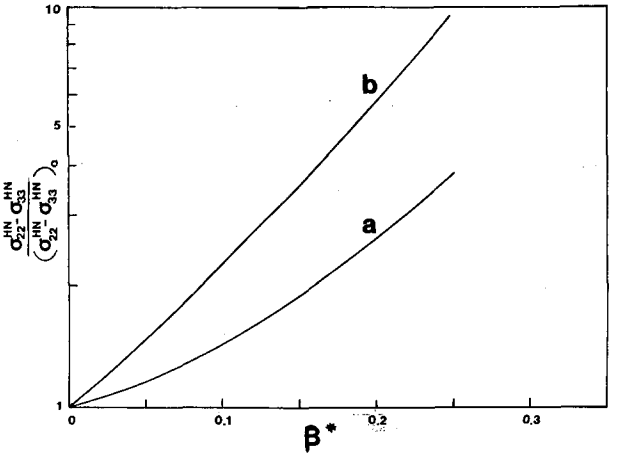

Fig. 8. Normalized second normal-stress difference, $(\sigma_{22}-\sigma_{33})^{HN}/(\sigma_{22}-\sigma_{33})_0^{HN}$, of a suspension of rodlike particles with small D in a second-order fluid as a function of β^* and r_e: (a) $r_e = 16$, (b) $r_e = 50$

magnitude smaller than $(\sigma_{11}^{HN}-\sigma_{22}^{HN})/\Phi\, g\, \eta_s$ but varies more appreciably as a function of β^* and r_e (see figures 7 and 8). Furthermore, $(\sigma_{11}^{HN}-\sigma_{22}^{HN})/\Phi\, g\, \eta_s$ has a negative contribution to the total first normal-stress difference, a behavior similar to what has been found by Kaloni and Stastna for spherical particles in a second-order fluid. The magnitude of $(\sigma_{11}^{HN}-\sigma_{22}^{HN})/\Phi\, g\, \eta_s$, however, will decrease with increasing β^* very slowly, as shown in figure 7. On the other hand, $(\sigma_{22}^{HN}-\sigma_{33}^{HN})/\Phi\, g\, \eta_s$ increases with increasing β^*.

4. Discussion and conclusion

In a dilute suspension, when the solvent is a Newtonian fluid, the Brownian rotational coefficient, D, for a rodlike particle can be estimated from Kirkwood's relation [31]

$$D = \frac{kT\ln(r_e)}{3\pi\eta_s L^3}, \tag{69}$$

where k is Boltzman's constant, T is the absolute temperature, η_s is the solvent viscosity, and L and r_e are the particle length and aspect ratio respectively. The diffusion coefficient depends strongly on L, and has a magnitude of $O(10^{-1})$ to $O(10)\,s^{-1}$ for the case of rodlike macromolecules in low viscosity solvents. Under a simple shear flow, when the shear rate is high enough to overcome the random diffusion force, the particles will start to orient themselves in the flow direction [36] leading to a decrease in the shear viscosity which will exhibit a shear-thinning behavior. The characteristic shear rate associated with this shear thinning has the same order of magnitude as D. For large rodlike particles, such as glass fibers of several hundred microns in length, the diffusion coefficient has typical values of about $10^{-8}\,s^{-1}$ or less (see Appendix B). For all practical shear flows imposed on the system, the particles will be oriented in the flow direction since the required shear rate to orient the particles will be of the order of $10^{-8}\,s^{-1}$ or smaller. One will therefore expect a constant shear viscosity within the accessible experimental range for these large rodlike particles in a Newtonian medium since no substantial orientation changes is possible by increasing the shear rate. This corresponds to the theoretical case of $\beta^* = 0$ which shows constant shear viscosity from $O(1)$ calculations, and the orientation picture, figure 4, which indicates that most of the particles are oriented in the flow direction. On the other hand, when large rodlike particles are suspended in a second-order fluid, our $O(1)$ calculations (for $\beta^* = 0$) indicate a shear-thinning behavior (figure 6). The fluid elasticity will orient the particles in their minimum energy dissipation state along the vorticity axis which will lower the system viscosity. When the shear rate g increases, β^* increases as g^2, and there are more particles shifting their orientation from the flow direction to the vorticity axis, and, consequently, the viscosity of the suspension is decreasing. The shift of orientation from along the flow to the vorticity axis has been shown in figure 5.

The cause of shear thinning when it occurs for rodlike suspensions in a Newtonian medium is very different from that expected for a suspension in a non-Newtonian fluid as described here. Only particles with strong Brownian diffusion (macromolecules) can show shear-thinning behavior in a Newtonian fluid due to the fact that the particles change their orientations from a random orientation to a quasi-alignment along

the flow direction as the shear rate is increased. No shear-thinning behavior for the large rodlike particle (with weak Brownian diffusion) in a Newtonian medium should be observed in the accessible experimental shear rate range. However, when the large particles are suspended in a second-order fluid, the shear-thinning behavior predicted by the theory is the result of the shift of particle alignment from the flow direction to the vorticity axis.

Faitel'son and Kovtun [37] have investigated a suspension of monodisperse fibers under simple shear flows. Different volume fractions (1%, 3%, and 5%) of Kapron fibers (aspect ratio 54) were suspended in an epoxy resin. Within their experimental temperature and shear rate range, the epoxy resin shows a constant shear viscosity; no normal stress measurements were reported. A shear-thinning behavior of the suspension is shown in their results, even for 1% volume concentration. We have analyzed their results for the 1% concentration suspension at 293 °K (see Appendix B). The rotational diffusion coefficient is of the order of $10^{-14}\,s^{-1}$ for these fibers. The shear viscosity starts thinning at a shear rate of about $0.5\,s^{-1}$. From the results shown in the Appendix B based on the model presented here, we note that a shear-thinning behavior at this shear rate for such a small diffusion coefficient would imply that the epoxy resin would have a zero-shear-rate second normal-stress coefficient of $\psi_2 = -10^{-7}$ dyne $\cdot$ s^2/cm^2. Although ψ_2 is very small and impossible to detect by available rheometry instruments, it may not have been zero; if that was the case, the observed shear thinning could have been caused by the combined effects of very small D and ψ_2.

It is noticed that the 1% volume concentration is already slightly beyond the dilute regime and in the semi-dilute concentration region [36] where $1/L^3 < \Phi < 1/dL^2$; hence particle interactions should be considered. However, Faitel'son and Kovtun report in their paper that separate fibers scarcely cross each other at this concentration. The shear thinning of the matrix itself at high shear rates is another possible reason for the shear-thinning behavior of the suspension at lower shear rates. However, the Kapron suspension discussed above shows a shear-thinning behavior at shear rates at least two orders of magnitude smaller than the maximum shear rate used on the pure matrix which behaved in a Newtonian fashion; it is very unlikely that the presence of the fibers would affect the relaxation mechanism of the matrix to this extent. A calculation for a suspension of particles in a corotational Jeffreys model fluid further supports this argument by showing that a new shear-thinning behavior will appear for the suspension at shear rates much smaller than the rates required to shear-thin the Jeffreys fluid. The corotational Jeffreys model is a non-Newtonian fluid model with a shear-thinning viscosity and non-zero first and second normal-stress differences which can be expressed as (Bird et al. [25])

$$\eta_s = \eta_0 \frac{1 + \lambda_1 \lambda_2 g^2}{1 + \lambda_1^2 g^2}, \tag{70}$$

$$\psi_1 = \frac{2\eta_0(\lambda_1 - \lambda_2)}{1 + \lambda_1^2 g^2}, \tag{71}$$

$$\psi_2 = \frac{-\eta_0(\lambda_1 - \lambda_2)}{1 + \lambda_1^2 g^2}, \tag{72}$$

where λ_1, λ_2 are two relaxation time parameters with the constraint $1/3 < \lambda_2/\lambda_1 < 1$. For $\lambda_1 g$, $\lambda_2 g \ll 1$, one has

$$\eta_s = \eta_0, \tag{73}$$

$$\psi_1 = 2\eta_0(\lambda_1 - \lambda_2), \tag{74}$$

$$\psi_2 = -\eta_0(\lambda_1 - \lambda_2), \tag{75}$$

and the fluid behaves as a second-order fluid under these conditions of low shear rates. We can therefore apply our theory to calculate the shear viscosity of the suspension in this regime. Here, we will choose $D = 2.0 \cdot 10^{-11}\,s^{-1}$, $\lambda_1 = 1.67 \cdot 10^{-3}\,s^{-1}$, $\lambda_2 = 0.4\lambda_1$, $\psi_2 = -10^{-3}$ dyne $\cdot$ s^2/cm^2, and $\eta_0 = 1$ poise (see Appendix B). The normalized viscosity curves for the pure corotational Jeffreys fluid and for the suspension are shown in figure 9. One can see that the suspension starts shear thinning much earlier than the pure matrix indicating that one would expect two independent and widely separated shear-thinning domains.

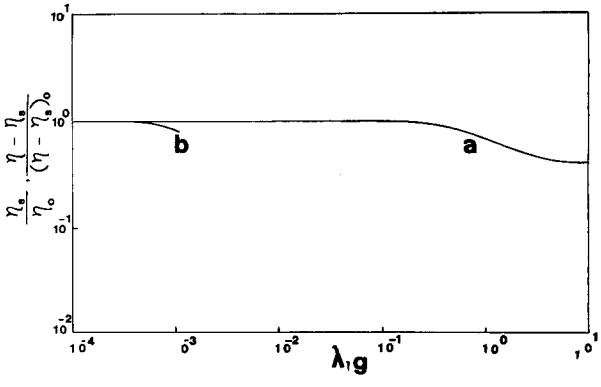

Fig. 9. Weak fluid elasticity effect on the shear-thinning behavior of viscosity of a suspension of large rodlike particles ($D = 2.0 \cdot 10^{-8}\,s^{-1}$, $r_e = 10^2$) in a corotational Jeffreys fluid ($\lambda_1 = 1.67 \cdot 10^{-3}\,s^{-1}$, $\lambda_2 = 0.4\lambda_1$, $\psi_2 = -10^{-3}$ dyne $\cdot$ s^2 $\cdot$ cm^{-2}, $\eta_0 = 1$ poise) at 300 °K: (a) corotational Jeffreys fluid, (b) suspension

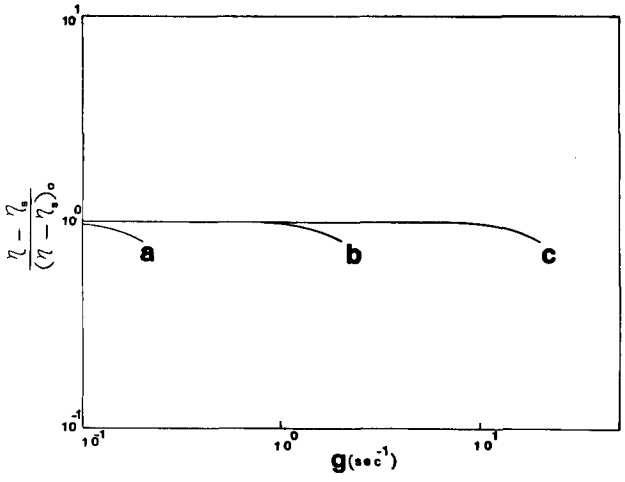

Fig. 10. Weak fluid elasticity, ψ_2 (dyne $\cdot$ s^2 $\cdot$ cm^{-2}), effect on the shear viscosity of a suspension of large rodlike particles ($D = 2 \cdot 10^{-12}$ s^{-1}, $r_e = 10^2$) in the second-order fluid ($\eta_s = 10^2$ poise): (a) $\psi_2 = -10^{-4}$, (b) $\psi_2 = -10^{-6}$, (c) $\psi_2 = -10^{-8}$

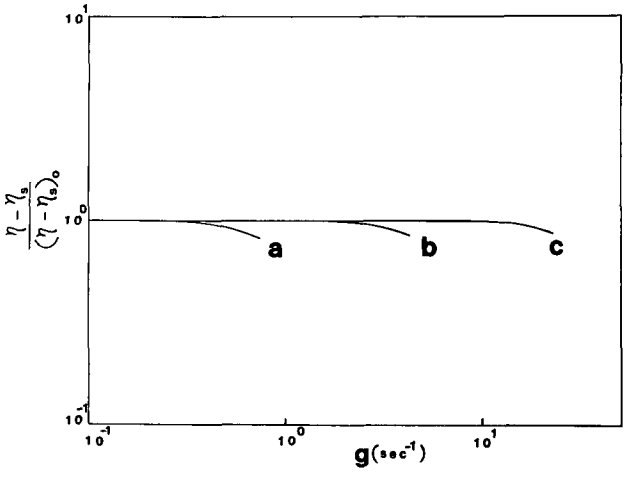

Fig. 11. Weak rotational diffusion coefficient effect on the shear viscosity of a suspension of large rodlike particles in a second-order fluid ($\eta_s = 10^2$ poise, $\psi_2 = -10^{-6}$ dyne $\cdot$ s^2 $\cdot$ cm^{-2}: (a) $D = 10^{-12}$ s^{-1}, $r_e = 50$, (b) $D = 10^{-10}$ s^{-1}, $r_e = 30$, (c) $D = 10^{-8}$ s^{-1}, $r_e = 16$

For a given particle size, when the fluid has a smaller ψ_2 value, the shear-thinning behavior of the suspension will start at a relatively higher shear rate required to build up enough elasticity force to bring the particles along the vorticity axis. This has been illustrated in figure 10. Similarly, for the same fluid, larger particle diffusion coefficients will shift the shear thinning point to higher shear rates as shown in figure 11.

In conclusion, for rodlike particles with weak Brownian diffusion in a second-order fluid, the orientation distribution of particles and rheological properties of the suspensions are functions of β^* which represents the ratio of the fluid elasticity effect to the particle Brownian diffusion effect. These two effects have been assumed here to be both weak but they can compete with each other to yield widely different distribution of orientations among the particles. One can combine the distribution function of orbits with the distribution function of phase angles for each orbit to give the full expression of the orientation distribution of particles in the suspension. Based on the obtained orientation distribution function, the rheological properties of the suspension were evaluated for different β^* values. Although the expressions used to calculate the rheological properties are only approximate ones for rodlike particles in a second-order fluid, interesting rheological behavior has been suggested by the theory; in particular, a shear-thinning viscosity of the suspension occurs as a result of the competing effects of weak fluid elasticity and weak Brownian diffusion of the particles.

Appendix A: The distribution function of orbits

A.1 Coordinate transformation

One can define the orbit constant, C, and phase angle, τ, in Jeffery's solution as:

$$C = \tan\theta \left(\frac{1}{r_e^2}\sin^2\phi + \cos^2\phi\right)^{1/2}, \tag{A.1}$$

$$\tau = \tan^{-1}\left(\frac{1}{r_e}\tan\phi\right). \tag{A.2}$$

On the other hand, θ and ϕ angles can be expressed in terms of C and τ

$$\theta = \tan^{-1}[C(\cos^2\tau + r_e^2\sin^2\tau)^{1/2}], \tag{A.3}$$

$$\phi = \tan^{-1}(r_e\tan\tau). \tag{A.4}$$

Based on eqs. (A.1–4), the following relations can be easily derived:

$$\theta_c = \left(\frac{\partial\theta}{\partial C}\right)_\tau = \frac{(\cos^2\tau + r_e^2\sin^2\tau)^{1/2}}{1 + C^2(\cos^2\tau + r_e^2\sin^2\tau)}, \tag{A.5}$$

$$\theta_\tau = \left(\frac{\partial\theta}{\partial\tau}\right)_C = \frac{C(r_e^2 - 1)\cos\tau\sin\tau}{(\cos^2\tau + r_e^2\sin^2\tau)^{1/2}[1 + C^2(\cos^2\tau + r_e^2\sin^2\tau)]}, \tag{A.6}$$

$$\phi_\tau = \left(\frac{\partial\phi}{\partial\tau}\right)_C = \frac{r_e}{\cos^2\tau + r_e^2\sin^2\tau}, \tag{A.7}$$

$$\left(\frac{\partial C}{\partial\theta}\right)_\phi = \frac{1}{\theta_c}, \tag{A.8}$$

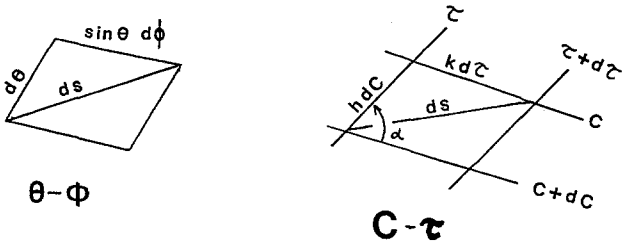

Fig. 12. The representation of a line segment in the two different coordinate systems: (θ, ϕ) and (C, τ)

$$\left(\frac{\partial C}{\partial \phi}\right)_\theta = -\frac{\theta_\tau}{\theta_c}\frac{(\cos^2\tau + r_e^2\sin^2\tau)}{r_e}, \tag{A.9}$$

$$\left(\frac{\partial \tau}{\partial \phi}\right)_\theta = \frac{1}{\phi_\tau}. \tag{A.10}$$

From figure 12, the line segment ds can be expressed as follows for the two different coordinate systems

$$ds^2 = d\theta^2 + \sin^2\theta\, d\phi^2$$
$$= \theta_C^2 dC^2 + 2\theta_C\theta_\tau dC\, d\tau + (\theta_\tau^2 + \sin^2\theta\,\phi_\tau^2)\, d\tau^2 . \tag{A.11}$$

Let

$$\theta_C = h \tag{A.12}$$

and

$$(\theta_\tau^2 + \sin^2\theta\,\phi_\tau^2)^{1/2} = k . \tag{A.13}$$

From the cosine law, eq. (A.11) can then be written as

$$ds^2 = h^2 dC^2 + k^2 d\tau^2 + 2hk\cos\alpha\, dC\, d\tau , \tag{A.14}$$

where $\cos\alpha = \theta_\tau/k$ and

$$\sin\alpha = \sin\theta\,\phi_\tau[\theta_\tau^2 + \sin^2\theta\,\phi_\tau^2]^{-1/2} . \tag{A.15}$$

Based on the above relations between the (θ, ϕ) and (C, τ) coordinate systems, eq. (25) can be transformed after algebraic manipulations to give in terms of C and τ:

$$\nabla\cdot\omega_0 f_0 = \frac{g r_e}{(r_e^2+1)}\left\{\frac{\partial f_0}{\partial \tau} - \frac{3C^2(r_e^2-1)\cos\tau\sin\tau}{[1+C^2(\cos^2\tau + r_e^2\sin^2\tau)]} f_0\right\} . \tag{A.16}$$

When $C \neq 0$, the above equation can be written as

$$\nabla\cdot\omega_0 f_0 = \frac{g}{r_e + r_e^{-1}}\frac{1}{hk\sin\alpha}\frac{\partial}{\partial\tau}(hk\sin\alpha\, f_0) = 0 , \tag{A.17}$$

where

$$hk\sin\alpha = \frac{C r_e}{[1 + C^2(\cos^2\tau + r_e^2\sin^2\tau)]^{3/2}} .$$

Integration of eq. (A.17) yields

$$(kh\sin\alpha) f_0 = l(C) . \tag{A.18}$$

Hence

$$f_0(C,\tau) = l(C)\, g(C,\tau) , \tag{A.19}$$

where $g(C,\tau) = 1/hk\sin\alpha$. On the other hand, when $C = 0$, eq. (A.16) can be written as

$$\nabla\cdot\omega_0 f_0 = \frac{g r_e}{r_e^2+1}\left\{\frac{\partial f_0}{\partial\tau}\right\} = 0 ,$$

therefore,

$$f_0(C,\tau) = l(C) . \tag{A.20}$$

A.2 Derivation of $l(C)$ in a second-order fluid

From eq. (30), one has

$$\oint(\omega_1 f_0)\cdot \boldsymbol{n}\, ds = \left(\frac{1}{\beta^* r_e^2}\right)\oint(\nabla f_0)\cdot \boldsymbol{n}\, ds , \tag{A.21}$$

where ω_1 is the additional contribution to the particle angular velocities caused by the fluid elasticity, and can be expressed as [21–22]

$$\omega_1 = -2\sin^3\theta\cos\phi\sin^2\phi\cos^2\phi\,\hat{\boldsymbol{\theta}} + \sin^3\theta\sin\phi\cos\phi(\sin^2\phi - \cos^2\phi)\,\hat{\boldsymbol{\phi}} . \tag{A.22}$$

$f_0(C,\tau)$ is of the same form as in the Newtonian case:

$$f_0(C,\tau) = l(C)\, g(C,\tau) . \tag{A.23}$$

One obtains after carrying out the integrations and simplifying the results,

$$\oint(\omega_1 f_0)\cdot \boldsymbol{n}\, ds = -l(C)\left\{\frac{2\pi(r_e^2+1)}{(r_e^2-1)^2}\frac{1}{C}[1 - \sqrt{(1+C^2)(1+r_e^2C^2)}] + \frac{\pi(r_e^2+1)^2}{(r_e^2-1)^2}C\right\} \tag{A.24}$$

and

$$\left(\frac{1}{\beta^* r_e^2}\right)\oint(\nabla f_0)\cdot \boldsymbol{n}\, ds = \left(\frac{1}{\beta^* r_e^2}\right)\pi\left\{[H(r_e)C^4 + K(r_e)C^2 + M(r_e)]\frac{dl}{dC} + \frac{1}{C}[2H(r_e)C^4 + (6 - K(r_e))C^2 - M(r_e)]l\right\} , \tag{A.25}$$

where $H(r_e) = r_e^2 + 1$,

$$K(r_e) = \frac{r_e^2}{4} + \frac{7}{2} + \frac{1}{4}r_e^2 , \tag{A.26}$$

and $M(r_e) = (r_e^2+1)/r_e^2$.

One obtains by equating eqs. (A.24) and (A.25):

$$\frac{dl}{dC} + \frac{2\tilde{H}C^4 + \left[6\left(\frac{1}{\beta^* r_e^2}\right) - \tilde{K} + \frac{(r_e^2+1)^2}{(r_e^2-1)^2}\right]C^2 - \left[\tilde{M} - \frac{2(r_e^2+1)}{(r_e^2-1)^2}\cdot(1 - \sqrt{(1+C^2)(1+r_e^2C^2)})\right]}{C[\tilde{H}C^4 + \tilde{K}C^2 + \tilde{M}]} l = 0$$

where

$$\tilde{H}=\left(\frac{1}{\beta^* r_e^2}\right)H(r_e)\,,\quad \tilde{K}=\left(\frac{1}{\beta^* r_e^2}\right)K(r_e)\,,\quad \text{and}\quad \tilde{M}=\left(\frac{1}{\beta^* r_e^2}\right)M(r_e)\,. \tag{A.27}$$

Eq. (A.27) can be solved by using a standard method which will give the solution as

$$l(C)=\text{const}\,e^{-\int P\,dC}\,, \tag{A.28}$$

where

$$P(C,r_e)=\frac{2\tilde{H}C^4+\left[\left(\frac{6}{\beta^* r_e^2}\right)-\tilde{K}+\frac{(r_e^2+1)^2}{(r_e^2-1)^2}\right]C^2-\left[\tilde{M}-\frac{2(r_e^2+1)}{(r_e^2-1)^2}\cdot\left(1-\sqrt{(1+C^2)\,(1+r_e^2C^2)}\right)\right]}{C(\tilde{H}C^4+\tilde{K}C^2+\tilde{M})}\,. \tag{A.29}$$

Then,

$$l(C)=\text{const}\,C^{J_1(r_e,\beta^*)}\left[\frac{HC^4+KC^2+M}{H}\right]^{J_2(r_e,\beta^*)}\left[\frac{2HC^2+K-\sqrt{K^2-4HM}}{2HC^2+K+\sqrt{K^2-4HM}}\right]^{J_3(r_e,\beta^*)}\cdot F_0(C)\cdot F_1(C)\cdot F_2(C)\,, \tag{A.30}$$

where $K^2-4HM>0$, $r_e\gg 1$, and $J_1(r_e\,\beta^*)$, $J_2(r_e,\beta^*)$, $J_3(r_e,\beta^*)$, and $F_0(C)$, $F_1(C)$, $F_2(C)$ are given in the text by eqs. (32–46).

Appendix B: Calculations for section 4

B.1 Rotational diffusion coefficient for short glass fiber

For $L=0.01$ cm, $r_e=100$, $\eta_s=1$ poise, $T=300$ K, and using

$$D=\frac{kT\ln r_e}{3\pi\eta_s L^3}$$

one obtains

$$D=\frac{(1.38\cdot 10^{-16}\,\text{erg/K})\,(300\,\text{K})\ln(100)}{(3)\,(3.1415)\,(1)\,(10^{-2}\,\text{cm}^2)^3}=2.0\cdot 10^{-8}\,\text{s}^{-1}\,.$$

B.2 Rotational diffusion coefficient for Kapron fiber in the Faitel'son and Kovtun's paper [37]

For $L=0.125$ cm, $d=0.0023$ cm, $r_e=54$, $\eta_s=330$ poise, $T=293$ K, one obtains

$$D=\frac{(1.38\cdot 10^{-16})\,(293)\ln(54)}{(3)\,(3.1415)\,(330)\,(0.125)^3}=2.66\cdot 10^{-14}\,\text{s}^{-1}\,.$$

The shear-thinning point, from their experimental results, is at $g\,a_T=100\,\text{s}^{-1}$, where $a_T=200$ at 293 K. Therefore $g=0.5\,\text{s}^{-1}$. If one assumes that $-\psi_2=10^{-7}$ dyne · s²/cm², one has then:

β^*	g	$(\eta-\eta_s)/(\eta-\eta_s)_0$
0.06252	0.358	0.9734 (C)
0.125	0.506	0.9302
0.1875	0.620	0.8775
0.22	0.671	0.8461
0.24	0.701	0.8248
0.248	0.713	0.8156
0.2499	0.715	0.8140

The shear-thinning point calculated from our theory is around the shear rate value of 0.5 s^{-1}, and would therefore be comparable with the experimental result with the choice of $-\psi_2\sim 10^{-7}$ dyne · s²/cm².

B.3 Corotational Jeffreys model

The rheological function of this model are given by [25]

$$\eta=\eta_0\frac{1+\lambda_1\lambda_2 g^2}{1+\lambda_1^2 g^2}\,,\quad \psi_1=\frac{2\eta_0(\lambda_1-\lambda_2)}{1+\lambda_1^2 g^2}\,,\quad \psi_2\frac{\eta_0(\lambda_1-\lambda_2)}{1+\lambda_1^2 g^2}\,,$$

where λ_1 and λ_2 are two relaxation time constants with the constraint $1/3<\lambda_2/\lambda_1<1$.

When $\lambda_1 g$, $\lambda_2 g\ll 1$, one has

$$\eta_s=\eta_0\,,\quad \psi_1=2\eta_0(\lambda_1-\lambda_2)\,,\quad \psi_2=-\eta_0(\lambda_1-\lambda_2)\,.$$

By choosing $\lambda_2/\lambda_1=0.4$ for the pure solvent, one has

$$\frac{\eta_s}{\eta_0}=\frac{1+0.4(\lambda_1 g)^2}{1+(\lambda_1 g)^2}\,.$$

One can plot η_s/η_0 vs. $\lambda_1 g$, which is shown in figure 9 in the text. For the suspension system, if $r_e=10^2$, $D=2.0\cdot 10^{-8}\,\text{s}^{-1}$, $\psi_2=-10^{-3}$ dyne · s²/cm², and $\eta_s=1$ poise, and taking $\lambda_1=1.67\cdot 10^{-3}\,\text{s}^{-1}$, $\lambda_2=6.68\cdot 10^{-4}\,\text{s}^{-1}$, and $\beta^*=-\psi_2/8\eta_s D r_e^2 g^2=0.625\,g^2$, one will have the following results:

β^*	g	$\lambda_1 g$	$(\eta_s-\eta)/(\eta-\eta_s)_0$
0.0625	0.316	$5.28\cdot 10^{-4}$	0.9734
0.125	0.447	$7.468\cdot 10^{-4}$	0.9302
0.1875	0.548	$9.147\cdot 10^{-4}$	0.8775
0.22	0.593	$9.908\cdot 10^{-4}$	0.8461
0.24	0.620	$1.035\cdot 10^{-3}$	0.8248
0.248	0.630	$1.052\cdot 10^{-3}$	0.8156
0.2499	0.632	$1.056\cdot 10^{-3}$	0.8140

The plot of $(\eta-\eta_s)/(\eta-\eta_s)_0$ vs. $\lambda_1 g$ is shown in figure 9 in the text.

Acknowledgement

This work is part of the Cornell Injection Molding Program supported by the National Science Foundation under Grant DMC-8507371.

References

1. Bright PF, Crowson RJ, Folkes MJ (1978) J Mater Sci 13:2497; Bright PF, Darlington MW (1981) Plastic and Rubber Process and Appl 1:139
2. Xavier SF, Tyagi D, Misra A (1982) Polym Composites 3:88
3. Pipes RB, McCullough RL, Taggart DB (1982) Polym Composites 3:34
4. Sanou M (1983) Technical Report 41. Cornell Injection Molding Program, Ithaca, NY
5. Jeffery GB (1922) Proc Roy Soc A 102:161
6. Karnis A, Goldsmith HL, Mason SG (1966) Can J Chem Engin 44:81
7. Okagawa A, Cox RG, Mason SG (1979) J Coll Interf Sci 71:11
8. Anczurowski E, Cox RG, Mason SG (1967) J Coll Interf Sci 23:547
9. Okagawa A, Mason SG (1973) J Coll Interf Sci 45:330
10. Ivanov Y, van de Ven TGM (1982) J Rheology 26:231
11. Cerda CM, Foister RT, Mason SG (1981) J Phys Chem 85:1075
12. Okagawa A, Cox RG, Mason SG (1973) J Coll Interf Sci 45:303
13. Ivanov Y, van de Ven TGM, Mason SG (1982) J Rheology 26:213
14. Zuzovski M, Priel Z, Mason SG (1980) J Coll Interf Sci 75:230
15. Leal LG, Hinch EJ (1971) J Fluid Mech 46:685
16. Folger F, Tucker III CL (1984) J Reinf Plast Compos 3:98
17. Saffman PG (1956) J Fluid Mech 1:540
18. Karnis A, Mason SG (1966) Trans Soc Rheol 10:571
19. Gauthier F, Goldsmith HL, Mason SG (1971) Rheol Acta 10:344
20. Batram E, Goldsmith HL, Mason SG (1975) Rheol Acta 14:776
21. Leal LG (1975) J Fluid Mech 69:305
22. Brunn P (1977) J Fluid Mech 82:529
23. Batchelor GK (1970) J Fluid Mech 41:545
24. Goodwin JW (1982) Colloidal dispersions, Dorset Press, Dorchester
25. Bird RB, Armstrong RC, Hassager O (1977) Dynamics of polymeric liquids, vol 1, Fluid Mechanics, John Wiley & Sons, New York
26. Hinch EJ, Leal LG (1973) J Fluid Mech 57:753
27. Hinch EJ, Leal LG (1972) J Fluid Mech 52:683
28. Wang MC, Uhlenbeck GE (1945) Rev Modern Physics 17:323
29. Trimble RH, Deutch JM (1971) J Stat Physics 3:149
30. Volkov VS, Vinogradov GB (1984) J Non-Newtonian Fluid Mech 15:29
31. Kirkwood JG, Auer PL (1951) J Chem Phys 19:281
32. Saito N (1951) J Phys Soc (Japan) 6:297
33. Brenner H (1972) Prog Heat Mass Transfer 5:89
34. Giesekus H (1962) Rheol Acta 2:50
35. Kaloni PN, Stastna V (1983) Polym Engin and Sci 23:465
36. Jain S, Cohen C (1981) Macromolecules 14:759
37. Faitel'son LA, Kovtun VP (1975) Polymer Mech 11:276

(Received July 8, 1986;
in revised form November 11, 1986)

Authors' addresses:

Prof. C. Cohen*)
School of Chemical Engineering
Cornell University
Ithaca, New York 14853
(U.S.A.)

Dr. B. Chung
GenCorp, Research Division
2990 Gilchrist Road
Akron, Ohio 44305
(U.S.A.)

Dr. W. Stasiak
Department of Mathematics and Mechanics
University of Warsaw
PL-00 901 Warsaw

*) To whom all correspondence should be addressed